An efficient beam element for the analysis of laminated composite beams of thin-walled open and closed cross sections

A.H. Sheikh, O.T. Thomsen

Accepted Manuscript

An efficient beam element for the analysis of laminated composite beams of thin-walled open and closed cross sections

A.H. Sheikh, O.T. Thomsen

PII: S0266-3538(08)00151-6
DOI: 10.1016/j.compscitech.2008.04.018
Reference: CSTE 4041

To appear in: *Composites Science and Technology*

Received Date: 20 September 2007
Revised Date: 14 April 2008
Accepted Date: 15 April 2008

Please cite this article as: Sheikh, A.H., Thomsen, O.T., An efficient beam element for the analysis of laminated composite beams of thin-walled open and closed cross sections, *Composites Science and Technology* (2008), doi: 10.1016/j.compscitech.2008.04.018

An efficient beam element for the analysis of laminated composite beams of thin-walled open and closed cross sections

A. H. Sheikh[*] and O. T. Thomsen[† I]

[*]*School of Civil, Environment and Mining Engineering, University of Adelaide*
North Terrace, Adelaide, SA 5005, Australia

[†]*Department of Mechanical Engineering, Aalborg University*
Pontopidanstraede 101, DK-9220, Aalborg, Denmark

Abstract

A condensed fully coupled beam element for thin-walled laminated composite beams having open or closed cross sections is presented. An analytical technique is used to derive the cross-sectional stiffness of the beam in a systematic manner considering all the deformation effects and their mutual couplings. An efficient finite element approximation is adopted for the transverse shear deformation, which has helped to conveniently implement the C^1 continuous formulation required by the torsional deformation due to incorporation of warping deformation. The performance of the element is tested through the solution of numerical examples involving open section I and channel (C) beams and closed section box beams under different loading conditions, and the obtained results are compared with model as well as experimental results available in literature.

***Keywords*:** Thin-walled laminated beams; Shear deformation; Warping deformations; Cross-sectional rigidities; Finite element approximation; Bending-torsion-extension-shear coupling

1. Introduction

The problem of modelling thin-walled laminated composite beam/beam like slender structures having open or closed cross section as one dimensional condensed beam elements has drawn a significant amount of attention of researchers over the last decades, and a number of investigations have been carried out to study the different aspects of this problem. A few representative studies relevant to the present context are given in [1-10]. One of the initial applications of composite beam theory was found in the analysis of helicopter rotor blades. It has subsequently been applied to the analysis of pultruded composite profiles and other applications, including the analysis of long and slender wind turbine blades made of composite materials.

The studies carried out so far may broadly be divided into two groups, based on the approach adopted for the evaluation of the constitutive matrix of the beam, defined as the cross-section stiffness coefficients. The first and most common approach is based on an analytical technique, while the other approach requires a two-dimensional finite element

[I] Author to whom correspondence should be addressed, Tel: +45 9940 9319, Fax: +45 9815 1675,
Email: ott@ime.aau.dk

analysis to obtain the cross-section stiffness matrix. Hodges and co-workers [3] pioneered the second approach, which is referred to as the so-called variational asymptotic beam section analysis (VABS). It is based on a method known as the variational asymptotic method (VAM) [11], where the three dimensional elasticity problem is systematically divided into a two dimensional cross-sectional problem, and a one dimensional beam problem (length direction). VABS has the advantage that beams having solid or thick-walled cross sections may be analyzed, where the three dimensional stress state can be extracted in the post processing stage. Opposed to this, the fully analytical approach may be preferred specifically for the analysis of beams with thin walled cross sections in order to avoid the additional two-dimensional finite element analysis required in VABS.

In this context it should be mentioned that Hodges and co-workers (e.g., Volovoi et al. [12], Volovoi and Hodges [13], Volovoi et al. [14], Volovoi and Hodges [15], Ye et al. [16]) further applied the concept introduced by the variational asymptotic method to two dimensional cross-sectional problem and derived closed-form expressions for the cross-sectional stiffness coefficients of thin-walled beams. As the resulting theory [12-16] evolved through rigorous mathematical treatments, it involves some additional terms including those for in-plane warping of the section, which is found to be important in some specific situations. Thus, the generality of the modelling has been enhanced in the asymptotic approach, but at the same time the mathematical formulation is very complex. However, the approach being a fully analytical one produced final results in the form of relatively simple closed-form expressions. The present approach proposes a fully coupled beam model which is significantly less mathematically complex, and which includes all effects except in-plane cross sectional warping.

In the present investigation, an analytical (closed-form) approach is adopted for the derivation of the cross-sectional stiffness matrix considering different effects and their coupling to yield a general formulation, which includes a torsional warping moment in addition to the classical (and well known) de St. Venant torsion contribution, an axial force, bi-axial bending moments and bi-axial transverse shear forces. In total this yields a 7x7 cross-sectional stiffness matrix. All the elements of this matrix are explicitly derived for open I and channel (or C) sections, and closed box section profiles. For the constitutive equation of any beam wall, defined locally, provision is kept to enable the specification of either plane stress conditions (zero normal stress along the wall profile, i.e. in the circumferential direction) or plane strain conditions (zero normal strain along the wall profile, i.e. in the circumferential direction).

For the finite element approximation of the beam element, the torsional deformation requires C^1 continuity of the twisting rotation due to incorporation of the out of plane warping deformation. This requirement is satisfied with the use of a Hermetian interpolation function considering the twisting rotation and its derivative with respect to the length coordinate as the nodal unknowns. The association of the derivative of the twisting rotation helps to impose warping restraints or warping free conditions by constraining or releasing this nodal unknown. At the same time the bending deformation requires C^0 continuity of the transverse displacements due to the incorporation of the transverse shear deformation of the beam walls. This requires a reduced integration technique for the evaluation of the stiffness matrix in order to avoid shear locking. As the bending deformation is not uncoupled from the other modes of deformation, including torsion, it is difficult to implement a C^0 formulation with a C^1 formulation having different orders of integration schemes. Lee [8] tried to solve the problem by an amended representation of the torsional deformation, so as to model it with a C^0 formulation like for bending deformation, but this involved a non-physical parameter in the formulation. Moreover, the C^0 formulation with reduced integration technique is susceptible to display inherent numerical disturbances like the occurrence of spurious modes.

Considering these aspects, the finite element implementation of the bending deformation in the present formulation is carried out with a different approach based on a concept proposed by the first author [17]. It does not require a reduced integration technique, and this effectively eliminates the problem described above. Based on this methodology a three node beam element, as shown in Fig. 1, has been developed, where the nodes at the two ends contain seven degrees of freedom (three translations, three rotations and the derivative of the twisting rotation), while the internal node contains five degrees of freedom (three translations and two bending rotations).

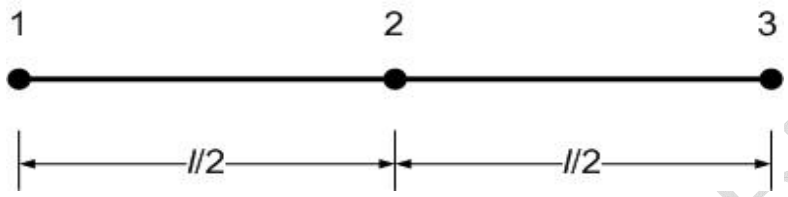

Fig. 1. Three node beam element

A computer program has been written in FORTRAN for the implementation of the proposed fully coupled composite beam element, which has been used to solve numerical examples of composite beams having open I and channel (C), and closed box sections. The results obtained in the form of deflections, angles of twist, and bending slopes are compared with analytical, experimental and/or other finite element analysis results available in literature. The results show a very good performance of the proposed element in terms of convergence and solution accuracy. The developed element is also utilized to derive some new results, which are presented for future references.

2. Formulation

Figure 2 shows a portion of the composite beam shell wall, with its local coordinate system *x*-*s*-*n*, the local displacement components, the global coordinate system *x*-*y*-*z* and finally the global beam displacement components.

In Fig. 2, *O* is the centroid, and *P* is the shear centre/pole of the beam section. The displacement components at the mid-plane of the shell wall in the local coordinate system (*x*-*s*-*n*) may be expressed in terms of the global displacement components of the beam [1] as

$$\bar{u} = U + y\theta_y + z\theta_z + \varphi\theta_x' \tag{1}$$

$$\bar{v} = V\cos\alpha + W\sin\alpha - r\theta_x \tag{2}$$

$$\bar{w} = -V\sin\alpha + W\cos\alpha + q\theta_x \tag{3}$$

where φ is the warping function, $\theta_y = -V' + \Psi_y$ (V' is the derivative of V with respect to x, and Ψ_y is the rotation of beam section about z for the transverse shear deformation) is the bending rotation of the beam section with respect to z, and $\theta_z = -W' + \Psi_z$ is the bending rotation of the beam section with respect to y.

For beams with closed cross sections, the effect of the warping function is not as significant as for open cross section beams, as has been nicely demonstrated by Ye et al. [16]. However, cross section warping has been included for both both closed and open cross section profiles

in order develop a general formulation for both type of beam profiles. Again, Volovoi and Hodges [15] have shown that the effect of in-plane warping is significant in some specific cases of closed section beams. However, this effect has not been incorporated in the present approach as mentioned earlier.

Considering the effect of shell bending and transverse shear deformation, the corresponding displacement components at a point away from the shell mid-plane may be expressed as

$$u = \bar{u} + n\left(-\frac{\partial \bar{w}}{\partial x} + \psi_{xn}\right) \tag{4}$$

$$v = \bar{v} + n\left(-\frac{\partial \bar{w}}{\partial s} + \psi_{sn}\right) \tag{5}$$

$$w = \bar{w} \tag{6}$$

where $\frac{\partial \bar{w}}{\partial x}$ and $\frac{\partial \bar{w}}{\partial s}$ are the bending rotations of the shell wall about x and s, respectively. Similarly, ψ_{xn} and ψ_{sn} are the shear rotations of the shell wall sections about s and x, respectively, for the transverse shear deformation. It is assumed that ψ_{sn} = 0, while ψ_{xn} may be expressed in terms of the corresponding global beam parameter as

$$\psi_{xn} = -\Psi_y \sin\alpha + \Psi_z \cos\alpha \tag{7}$$

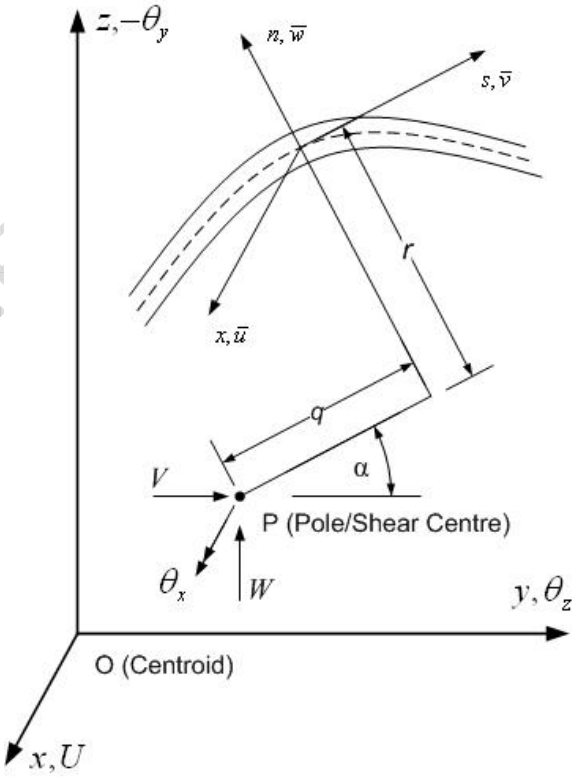

Fig. 2. Cross-section of a portion of a shell wall of the thin-walled composite beam with local and global coordinate systems and displacement components

With the above equations, the displacement components at any point within the shell wall may be expressed in terms of the global beam displacement components as

$$u = U + \left(y - n\sin\alpha\right)\theta_y + \left(z + n\cos\alpha\right)\theta_z + \left(\varphi - nq\right)\theta_x' \tag{8}$$

$$v = V\cos\alpha + W\sin\alpha - \left(r + n\right)\theta_x \tag{9}$$

$$w = -V\sin\alpha + W\cos\alpha + q\theta_x \tag{10}$$

The strain components at the corresponding point in the local axis system (*x*-*s*-*n*) may be expressed as

$$\left\{\hat{\varepsilon}\right\} = \begin{Bmatrix} \varepsilon_x \\ \varepsilon_s \\ \varepsilon_{xs} \\ \varepsilon_{xn} \\ \varepsilon_{sn} \end{Bmatrix} = \begin{Bmatrix} \dfrac{\partial u}{\partial x} \\ \dfrac{\partial v}{\partial s} \\ \dfrac{\partial u}{\partial s} + \dfrac{\partial v}{\partial x} \\ \psi_{xn} \\ \psi_{sn} \end{Bmatrix} \tag{11}$$

Assuming the normal strain component ε_s to be zero (plane strain condition), or the normal stress component σ_s to be zero (plane stress condition), the reduced strain vector may be expressed in terms of the global displacement parameters with the help of the above Eqs. (7-10) as

$$\left\{\varepsilon\right\} = \begin{Bmatrix} \varepsilon_x \\ \varepsilon_{xs} \\ \varepsilon_{xn} \end{Bmatrix} = \begin{Bmatrix} \left(\dfrac{\partial u}{\partial x}\right) \\ \left(\dfrac{\partial u}{\partial s} + \dfrac{\partial v}{\partial x}\right) \\ \psi_{xn} \end{Bmatrix} = \begin{Bmatrix} U' + \left(y - n\sin\alpha\right)\theta_y' + \left(z + n\cos\alpha\right)\theta_z' \\ \qquad + \left(\varphi - nq\right)\theta_x'' \\ \Psi_y\cos\alpha + \Psi_z\sin\alpha - \left(2n + r - \dfrac{\partial\varphi}{\partial s}\right)\theta_x' \\ -\Psi_y\sin\alpha + \Psi_z\cos\alpha \end{Bmatrix} \tag{12}$$

The above equation can further be rearranged in matrix form as

$$\{\varepsilon\}=\begin{bmatrix} 1 & 0 & 0 \\ y-n\sin\alpha & 0 & 0 \\ z+n\cos\alpha & 0 & 0 \\ \varphi-nq & 0 & 0 \\ 0 & -\left(2n+r-\varphi_{,s}\right) & 0 \\ 0 & \cos\alpha & \sin\alpha \\ 0 & -\sin\alpha & \cos\alpha \end{bmatrix}\begin{Bmatrix} U' \\ \theta_y' \\ \theta_z' \\ \theta_x'' \\ \theta_x' \\ V'+\theta_y \\ W'+\theta_z \end{Bmatrix}=[H]\{\bar{\varepsilon}\} \tag{13}$$

Considering the transverse shear deformation of the laminated shell wall [18], the stress strain relationship at any point within a lamina of the laminated shell wall in the local coordinate system parallel to *x*-*s*-*n* may be expressed as

$$\begin{Bmatrix} \sigma_x \\ \sigma_s \\ \sigma_{xs} \\ \sigma_{xn} \\ \sigma_{sn} \end{Bmatrix}=\begin{bmatrix} \overline{Q}_{11} & \overline{Q}_{12} & \overline{Q}_{16} & 0 & 0 \\ \overline{Q}_{21} & \overline{Q}_{22} & \overline{Q}_{26} & 0 & 0 \\ \overline{Q}_{61} & \overline{Q}_{62} & \overline{Q}_{66} & 0 & 0 \\ 0 & 0 & 0 & \overline{Q}_{55} & \overline{Q}_{54} \\ 0 & 0 & 0 & \overline{Q}_{45} & \overline{Q}_{44} \end{bmatrix}\begin{Bmatrix} \varepsilon_x \\ \varepsilon_s \\ \varepsilon_{xs} \\ \varepsilon_{xn} \\ \varepsilon_{sn} \end{Bmatrix} \tag{14}$$

Assuming $\varepsilon_s = 0$ or $\sigma_s = 0$ along with $\psi_{ns} = 0$, the above equation reduces to

$$\begin{Bmatrix} \sigma_x \\ \sigma_{xs} \\ \sigma_{xn} \end{Bmatrix}=\begin{bmatrix} \tilde{Q}_{11} & \tilde{Q}_{16} & 0 \\ \tilde{Q}_{61} & \tilde{Q}_{66} & 0 \\ 0 & 0 & \tilde{Q}_{55} \end{bmatrix}\begin{Bmatrix} \varepsilon_x \\ \varepsilon_{xs} \\ \varepsilon_{xn} \end{Bmatrix} \tag{15}$$

where $\tilde{Q}_{11}=\overline{Q}_{11}$, $\tilde{Q}_{16}=\overline{Q}_{16}$, $\tilde{Q}_{66}=\overline{Q}_{66}$ and $\tilde{Q}_{55}=\overline{Q}_{55}$ for the plane strain ($\varepsilon_s = 0$) condition; and $\tilde{Q}_{11}=\overline{Q}_{11}-\overline{Q}_{12}\overline{Q}_{12}/\overline{Q}_{22}$, $\tilde{Q}_{16}=\overline{Q}_{16}-\overline{Q}_{12}\overline{Q}_{26}/\ \overline{Q}_{22}$, $\tilde{Q}_{66}=\overline{Q}_{66}-\overline{Q}_{16}\overline{Q}_{16}/\overline{Q}_{22}$ and $\tilde{Q}_{55}=\overline{Q}_{55}$ for the plane stress ($\sigma_s = 0$) condition.

Using Eqs. (13) and (15), the strain energy of the system can be written as

$$\tilde{U}=\frac{1}{2}\int\{\varepsilon\}^T\{\sigma\}dv=\frac{1}{2}\int\{\bar{\varepsilon}\}^T[F]\{\bar{\varepsilon}\}dx \tag{16}$$

where $[F]=\int\int[H]^T\left[\tilde{Q}\right][H]dsdn=\int\left(\int[H]^T\left[\tilde{Q}\right][H]dn\right)ds=\int[C]ds$

All the elements of the cross-sectional stiffness matrix [F] are explicitly derived for open I and channel (C) sections as well as for closed box section profiles. The explicit expressions for the different elements of the matrix [F] are presented in Appendix B, C and D for I section, channel section (C) and box section, respectively. The matrix [C] is common for all the considered cross-sections, and its elements are presented in Appendix A. For this purpose the warping function φ used in the above equations are taken as

$$\varphi = \int r ds - 2A_c \delta_s / \delta \tag{17}$$

where $\delta_s = \int \frac{ds}{\tilde{Q}_{66}}$, $\delta = \oint \frac{ds}{\tilde{Q}_{66}}$ and A_c is the cross-sectional area enclosed by the mid-plane contour in the case of beams having closed section profiles. For an open section profile, the warping function may be simply obtained by dropping the second term associated with secondary warping, thus giving as $\varphi = \int r ds$.

For the one dimensional finite element implementation, a quadratic approximation has been adopted for the axial deformation, which follows a Lagrangian type formulation. The torsional deformation is based on a Hermetian formulation as mentioned earlier, where a cubic approximation has been adopted. The approximation of the bending deformation coupled with transverse shear deformation is based on the concept proposed by Sheikh [17]. Based on this the field variables are approximated as follows

$$U = a_1 + a_2 x + a_3 x^2 \tag{18}$$

$$V = a_4 + a_5 x + a_6 x^2 + a_7 x^3 \tag{19}$$

$$W = a_8 + a_9 x + a_{10} x^2 + a_{11} x^3 \tag{20}$$

$$\Psi_y = a_{12} + a_{13} x \tag{21}$$

$$\Psi_z = a_{14} + a_{15} x \tag{22}$$

$$\theta_x = a_{16} + a_{17} x + a_{18} x^2 + a_{19} x^3 \tag{23}$$

It should be noted that Ψ_y and Ψ_z are adopted as the field variables instead of θ_y and θ_z, which are usually used in a typical C^0 formulation. However, the corresponding nodal unknowns are interestingly θ_y and θ_z, and these are not simply the field variables Ψ_y and Ψ_z. Now, with the help of Eqs. (19-22), the bending rotations θ_y and θ_z may be expressed as

$$\theta_y = a_{12} + a_{13} x - a_5 - 2a_6 x - 3a_7 x^2 \tag{24}$$

$$\theta_z = a_{14} + a_{15} x - a_9 - 2a_{10} x - 3a_{11} x^2 \tag{25}$$

The unknowns ($a_1, a_2, a_3, \cdots a_{19}$) in the above Eqs. (18-23) are expressed in terms of the nodal displacement vector $\{\delta\}$ after substitution of U (18), V (19), W (20), θ_y (24) and θ_z (25) at all the three nodes of the beam element (see Fig. 1); and θ_x (23) and its derivative θ'_x at the two external nodes as

$$\{\delta\} = [R]\{a\} \text{ or } \{a\} = [R]^{-1}\{\delta\} \tag{26}$$

where $\{a\} = [a_1 \quad a_2 \quad a_3 \quad \cdots \quad a_{18} \quad a_{19}]^T$, $\{\delta\} = [\, U_1 \quad V_1 \quad W_1 \quad \theta_{x1} \quad \theta_{y1} \quad \theta_{z1} \quad \theta'_{x1}$

$U_2 \quad V_2 \quad W_2 \quad \theta_{y2} \quad \theta_{z2} \quad U_3 \quad V_3 \quad W_3 \quad \theta_{x3} \quad \theta_{y3} \quad \theta_{z3} \quad \theta'_{x3}\big]^T$, and the matrix [*R*] having an order of 19x19 contains the element nodal coordinates.

The generalized strain vector $\{\bar{\varepsilon}\}$ in Eq. (13) may be expressed in terms of $\{a\}$ using Eqs. (18-23) as

$$\{\bar{\varepsilon}\} = \begin{Bmatrix} U' \\ \theta'_y \\ \theta'_z \\ \theta''_x \\ \theta'_x \\ V' + \theta_y \\ W' + \theta_z \end{Bmatrix} = \begin{Bmatrix} U' \\ -V'' + \Psi'_y \\ -W'' + \Psi'_z \\ \theta''_x \\ \theta'_x \\ \Psi'_y \\ \Psi'_z \end{Bmatrix} = [S]\{a\} \tag{27}$$

where the matrix [*S*] having an order of 7x19 is a function of *x*. The strain vector $\{\bar{\varepsilon}\}$ can be finally expressed in terms of the nodal displacement vector $\{\delta\}$ using Eq. (26) as

$$\{\bar{\varepsilon}\} = [S][R]^{-1}\{\delta\} = [B]\{\delta\} \tag{28}$$

With the above equation, the strain energy (16) of the system may be expressed as

$$\tilde{U} = \frac{1}{2}\{\delta\}^T \int [B]^T [F][B] dx \{\delta\} = \frac{1}{2}\{\delta\}^T [K]\{\delta\} \tag{29}$$

where [*K*] is the element stiffness matrix. Using Eq. (20) and Eq. (26), the element load vector due to a distributed transverse load of intensity *q* acting in the direction of *z* may be expressed as

$$\{P\} = [R]^{-T} \int q \left[S_q\right]^T dx \tag{30}$$

where the row matrix $\left[S_q\right]$ having an order of 19 is function of *x*. The integrations involved in the evaluation of the element stiffness matrix [*K*] and the load vector {*P*} are carried out numerically following the Gauss quadrature technique.

3. Results and discussions

In the following a number of numerical examples involving composite beams with I, channel (C) or box cross sections are analysed using the proposed element, and the results obtained are compared with analytical, experimental and/or numerical results available in literature for most of the cases. The analyses are usually based on plane stress conditions, unless specified otherwise. In all examples the beam walls are assumed to be constituted by identical layers of the same thickness, but the layers may have different orientations. The geometry of the beam sections are defined in terms of their centre line dimensions.

3.1. Simply supported I beam subjected to uniformly distributed transverse load

A 2.5m long open section I beam simply supported at its two ends, and subjected to a uniformly distributed transverse load of 1kN/m along the web of the beam, is analysed using the proposed element. The beam has a depth of 50mm, a flange width of 50mm and same thickness (2.08mm) for the flanges and the web. The study is made with different symmetrical stacking sequences, where the flanges and the web are having identical lay-ups for all cases. The material properties of the layers are: E_1 = 53.78GPa, E_2 = 17.93GPa, G_{12} = 8.96GPa, G_{13} = 8.96GPa, G_{23} = 3.45GPa, ν_{12} = 0.25. The analysis is carried out assuming both plane stress and plane strain conditions. The values of deflection at the centre of the beam and the bending slope at its supports obtained in the present analysis are presented in Table 1 and Table 2, respectively. The results for the deflections are compared with those of Lee [8] and Lee and Lee [19] in Table 1. Lee [8] considered the effect of transverse shear deformation, whereas the study of Lee and Lee [19] is based on classical lamination theory. In both the studies [8, 19], one dimensional finite element analysis has been applied after obtaining the cross-sectional stiffness matrix analytically. For the validation of the results in [8, 19], the beam structure was analysed using ABAQUS [20], where the S9R5 shell element was used to model the composite beam. The results produced by ABAQUS [20] are also included in Table 1. The table shows an excellent agreement between the predictions of the present model and the results of the other models mentioned, especially the results of Lee [8]. Moreover, the present results based on plane stress conditions are found to be closer to the results produced by ABAQUS [20] than the results in [8], [19]. It is further observed that in all cases convergence of the results was achieved using only two elements with the approach proposed herein.

Table 1
Deflection w (cm) at the centre of the simply supported I beam

Stacking sequence	$[0/0]_{4S}$	$[15/-15]_{4S}$	$[30/-30]_{4S}$	$[45/-45]_{4S}$	$[60/-60]_{4S}$	$[75/-75]_{4S}$	$[0/90]_{4s}$
Present ($\sigma_s = 0$) - 2†	6.264	6.929	9.320	13.45	17.00	18.46	9.387
Present ($\sigma_s = 0$) - 4†	6.264	6.929	9.320	13.45	17.00	18.46	9.387
Present ($\varepsilon_s = 0$) - 2†	6.134	6.640	8.309	11.37	15.15	17.68	9.192
Present ($\varepsilon_s = 0$) - 4†	6.134	6.640	8.309	11.37	15.15	17.69	9.192
Lee [8] ($\sigma_s = 0$)	6.259	6.923	9.314	13.45	16.99	18.45	9.381
Lee [8] ($\varepsilon_s = 0$)	6.129	6.637	8.307	11.36	15.15	17.68	9.189
Lee and Lee [19] ($\sigma_s = 0$)	6.233	6.899	9.290	13.42	16.96	18.41	9.299
Lee and Lee [19] ($\varepsilon_s = 0$)	6.103	6.610	8.281	11.34	15.12	17.64	9.153
ABAQUS [20]	6.340	6.989	9.360	13.48	17.02	18.49	9.400

† Number of elements

Table 2
Bending rotation θ_z x 100 (rad) at the support of the simply supported I beam

Stacking sequence	$[0/0]_{4S}$	$[15/-15]_{4S}$	$[30/-30]_{4S}$	$[45/-45]_{4S}$	$[60/-60]_{4S}$	$[75/-75]_{4S}$	$[0/90]_{4s}$
Present ($\sigma_s = 0$) - 2†	7.978	8.830	11.89	17.18	21.71	23.57	11.97
Present ($\sigma_s = 0$) - 4†	7.978	8.830	11.89	17.18	21.71	23.57	11.97
Present ($\varepsilon_s = 0$) - 2†	7.812	8.461	10.60	14.52	19.35	22.58	11.72
Present ($\varepsilon_s = 0$) - 4†	7.812	8.461	10.60	14.52	19.35	22.58	11.72

† Number of elements

3.2. Clamped box beam subjected to uniformly distributed transverse load

A box beam clamped at both ends, and subjected to uniformly distributed transverse load of 6.5kN/m along the mid-plane of one of the webs, is analysed using the proposed element assuming both plane stress and plane strain conditions. The beam is assumed to be free from axial and warping restraints at the supports. The beam is 1.0 m long, 70 mm deep and 50 mm wide, and all the beam walls are 2 mm thick having a stacking sequence of $(45/-45)_2/(0/0)_6/(45/-45)_2$. The material properties assumed for all layers are: E_1 = 148.0 GPa, E_2 = 9.65 GPa, $G_{12} = G_{13} = G_{23}$ = 4.55 GPa, ν_{12} = 0.3. The values of the deflection and angle of twist at the centre of the beam obtained in the present analysis are presented in Table 3, along with results obtained by Kollar and Springer [6] assuming plane strain conditions, and Vo and Lee [21] assuming both plane stress and plane strain conditions. Kollar and Springer [6] solved the problem analytically (closed form), while Vo and Lee [21] applied one dimensional finite element analysis after obtaining the cross-sectional stiffness matrix analytically. As both of the studies [6, 21] did not consider the effect of transverse shear deformation, the present analysis was also carried out with very high values of transverse shear moduli ($G_{13} = G_{23} = G_{12}$ x 10^6), and the results obtained are included in Table 3 (marked ‡). The results show a significant effect of the transverse shear deformation and a wide variation of the values of torsional rotation obtained on the basis of plane stress and plane strain assumptions. The table shows that the convergence of the present finite element formulation is very good. It also shows a good agreement between the results obtained by the different techniques having similar basis.

Table 3
Deflection and angle of twist at the centre of the clamped box beam

	w x 10^4 (m)			θ_x x 10^3 (rad)		
Number of elements	2	4	6	2	4	6
Present † ($\sigma_s = 0$) - 2♠	7.811	7.811	7.811	6.705	6.703	6.703
Present † ($\varepsilon_s = 0$) - 2♠	5.779	5.779	5.779	2.755	2.754	2.754
Present ‡ ($\sigma_s = 0$) - 2♠	4.940	4.940	4.940	6.705	6.703	6.703
Present ‡ ($\varepsilon_s = 0$) - 2♠	4.378	4.378	4.378	2.755	2.754	2.754
Vo and Lee [21] ($\sigma_s = 0$)		4.940			6.427	
Vo and Lee [21] ($\varepsilon_s = 0$)		4.380			2.678	
Kollar and Springer [6] ($\varepsilon_s = 0$)		4.880			2.760	

† $G_{13} = G_{12}$, ‡ $G_{13} = G_{23} = G_{12}$, x 10^6, ♠ Number of elements

3.3. Cantilever I beam subjected to tip transverse load with restrained warping

A 0.762 m (30 inch) long cantilever I beam subjected to a transverse unit load of 4.4482 N (1.0 lb) at the free end is analysed using the proposed element assuming restrained warping at both ends. The beam has a depth of 12.7 mm (0.5 inch), a flange width of 25.4 mm (1.0 inch) and the same thickness of 1.016 mm (0.04 inch) is assumed for the flanges and the web. The stacking sequence of the flange is 0/90/0/90/90/0/15/15, while that of the web is 0/90/0/90/90/0/90/0. The assumed material properties are: E_1 = 141.96 GPa (20.59 x10^6 Psi), E_2 = 9.7906 GPa (1.42 x10^6 Psi), $G_{12} = G_{13} = G_{23}$ = 6.1363 GPa (0.89 x10^6 Psi), ν_{12} = 0.42.

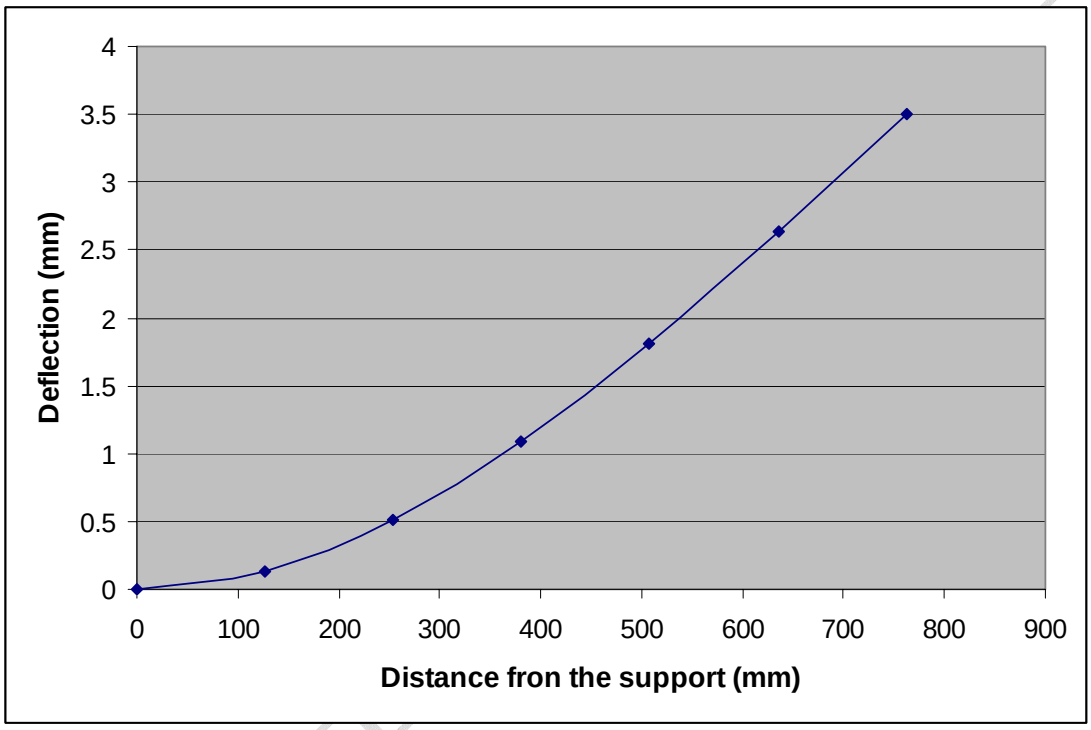

Fig. 3. Variation of deflection of the I beam

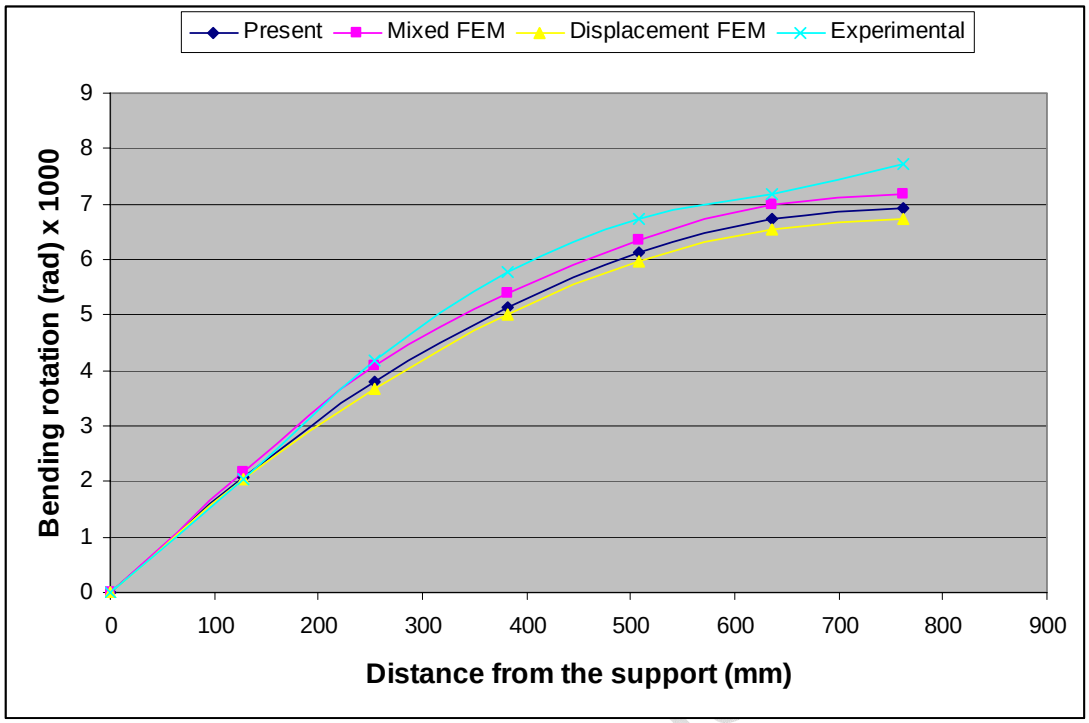

Fig. 4. Variation of bending slope of the I beam

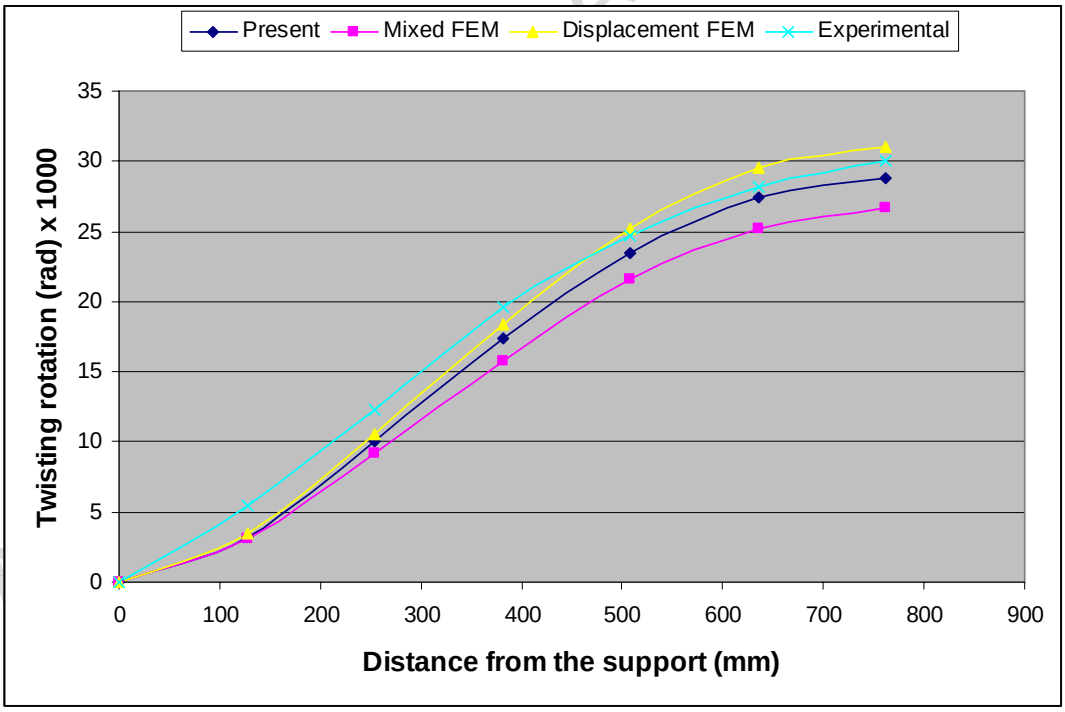

Fig. 5. Variation of twisting rotation of the I beam

The variation of deflection, bending slope and twisting rotation along the length of the beam are plotted in Fig. 3, Fig. 4 and Fig. 5, respectively. The results for the bending slope and twisting rotation are compared with the numerical results of Jung et al. [5] and the experimental results of Chandra and Chopra [22] in Fig. 4 and Fig. 5. Jung et al. [5] has

produced results based on a mixed formulation, as well as on the displacement formulation of Smith and Chopra [23], where one dimensional finite element has been applied after obtaining the cross-sectional stiffness matrix analytically. The figures show an excellent agreement between the results of the approach proposed herein and the results given in [5, 22, 23].

3.4. Cantilever box beam subjected to tip transverse load/twisting moment

A 0.762 m (30 inch) long cantilever box beam having a depth of 12.7 mm (0.5 inch), a width of 23.444 mm (0.923 inch) and assuming the same thickness of 0.762 mm (0.03 inch) for all the walls consisting of 6 layers is analysed using the proposed element. The assumed loading is either a unit transverse load of 4.4482 N (1.0 lb) or a unit twisting moment of 0.11299 Nm (1.0 lb-inch) applied at the free end. The stacking sequence of the top and bottom walls is $(45/45)_3$, while that of the left and right walls is $(45/-45)_3$. The material properties of all layers are assumed to be identical and the same as those adopted in the previous example (I beam). The variation of the bending slope and twisting rotation along the length of the beam are plotted in Fig. 6 to Fig. 9 along with the analytical and experimental results of Chandra et al. [2], and the finite element results of Stemple and Lee [24]. The results of the different methods are found to be in excellent agreement.

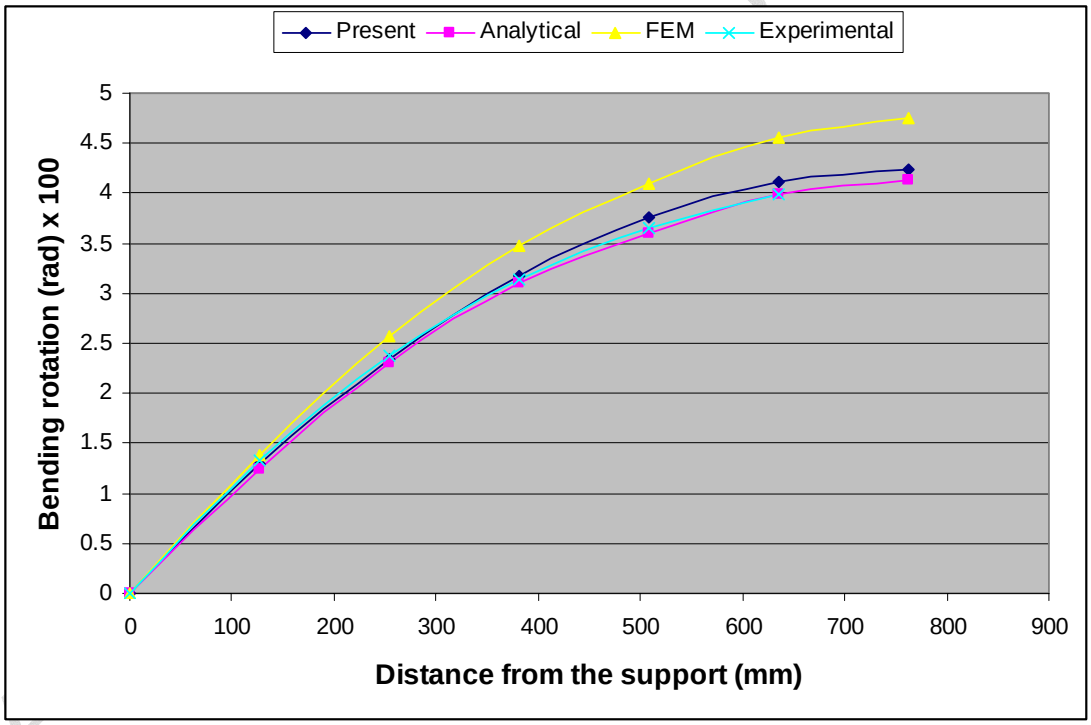

Fig. 6. Variation of bending slope of the box beam under a transverse load at the tip

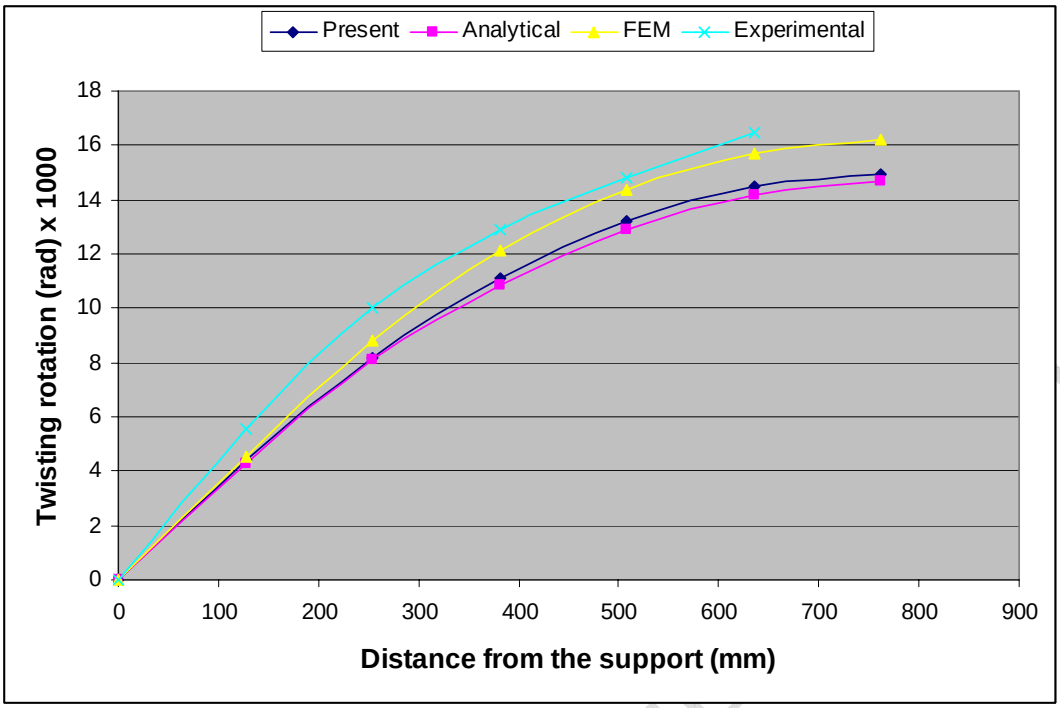

Fig. 7. Variation of twisting rotation of the box beam under a transverse load at the tip

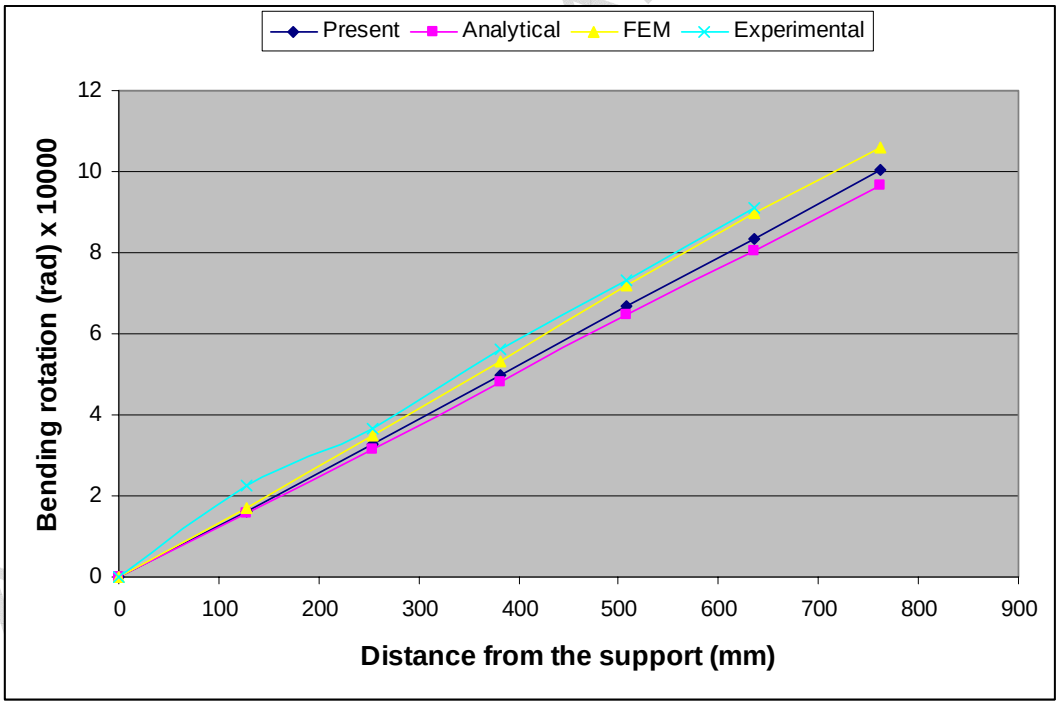

Fig. 8. Variation of bending slope of the box beam under a twisting moment at the tip

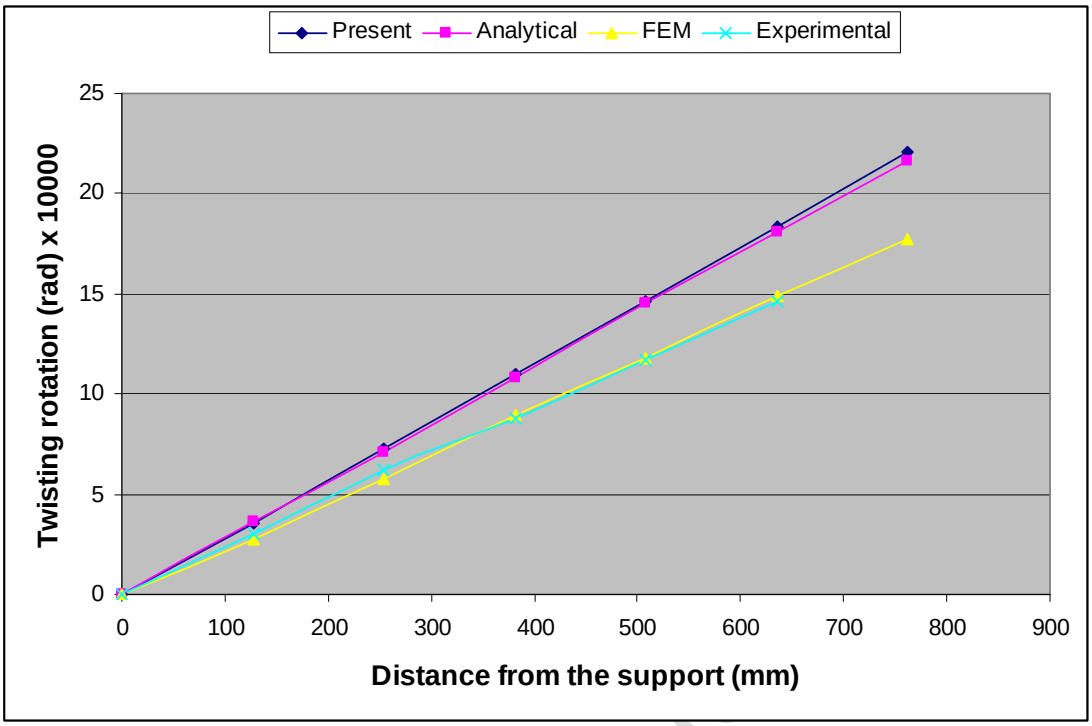

Fig. 9. Variation of twisting rotation of the box beam under a twisting moment at the tip

3.5. A channel beam clamped at one end and simply supported at the other end

A 2.5 m long beam having a channel (C) section clamped at one end and simply supported at the other end is analysed using the proposed element. The channel section has a depth of 50 mm, a width of 25 mm and the same thickness of 2.08 mm for all the walls consisting of 16 layers. The layers are having identical orientation, which is varied from 0^0 to 90^0 with an interval of 15^0. The material properties of the layers are: E_1 = 53.78GPa, E_2 = 17.93GPa, G_{12} = 8.96GPa, G_{13} = 8.96GPa, G_{23} = 3.45GPa, ν_{12} = 0.25. The beam is subjected to a unit twisting moment 1.0 Nm at the simply supported end.

Table 4

Maximum angle of twist of a beam having a channel section

Stacking sequence	$[0]_{16}$	$[15]_{16}$	$[30]_{16}$	$[45]_{16}$	$[60]_{16}$	$[75]_{16}$	$[90]_{16}$
Present Element – 2†	0.2441	0.2195	0.1934	0.2029	0.2394	0.2793	0.2967
Present Element – 4†	0.2444	0.2198	0.1939	0.2038	0.2405	0.2804	0.2978
Present Element – 6†	0.2444	0.2199	0.1940	0.2038	0.2405	0.2805	0.2979
Present Element – 8†	0.2444	0.2199	0.1940	0.2038	0.2406	0.2805	0.2979
Closed form solution [25]	0.2444	0.2199	0.1940	0.2038	0.2406	0.2805	0.2979
Finite Element - I [25] – 1†	0.2444	0.2199	0.1940	0.2038	0.2406	0.2805	0.2979
Finite Element -II [25] – 4†	0.2444	0.2198	0.1939	0.2038	0.2404	0.2804	0.2978
ABAQUS [20]	0.2459	0.2250	0.2011	0.2090	0.2427	0.2795	0.2952

† Number of elements

The results for the angle of twist at the simply supported end obtained by the proposed element are presented with those obtained by Kim et al. [25] in Table 4. Kim et al. [25] applied an analytical technique (closed form) and two different finite element models to analyse the problem. They have also analysed the structure using ABAQUS [20] where the structure is modelled with shell elements. Table 4 shows that the results obtained from the different sources are showing an excellent agreement with the predictions of the coupled beam element proposed herein. Moreover, Table 4 also shows a very good convergence of the results obtained by the proposed element.

4. Conclusions

A fully coupled beam element has been developed for the analysis of thin-walled laminated composite beams of open and closed cross sections including axial displacement, torsion, out of plane warping, bi-axial bending and transverse shear deformations. The constitutive equations of the beam element are derived analytically considering the coupling of all the modes of deformation, i.e. the beam model is fully coupled. The resulting composite beam theory is applied to laminated composite beams of open I and channel cross sections, as well as to laminated composite beams of closed box cross sections. The incorporation of transverse shear deformations demands a C^0 formulation for the one dimensional finite element approximation of the bending deformations, while the torsional deformation demands a C^1 formulation for the incorporation of out-of-plane warping. The difficulty in implementing both formulations in the present coupled problem is successfully overcome by adopting an efficient approach for the finite element approximation of the bending deformations. Numerical examples of composite open and closed cross section beams having different load and boundary conditions are analysed using the proposed element. The results obtained are compared with analytical, experimental and/or other finite element results available in literature, and the comparisons show a very good performance of the proposed fully coupled beam element. In addition to the comparative studies, some new results are also presented for future references.

Acknowledgement

The work presented was carried out as part the Innovation Consortium “Integrated Design and Processing of Lightweight Composite and Sandwich Structures” (abbreviated “KOMPOSAND”) funded by the Danish Ministry of Science, Technology and Innovation and the industrial partners Composhield A/S, DIAB ApS (DIAB Group), Fiberline Composites A/S, LM Glasfiber A/S and Vestas Wind Systems A/S. The support received is gratefully acknowledged.

References

[1] Bauld NR, Tzeng LS. A Vlasov theory for fiber-reinforced beams with thin-walled open cross section. International Journal of Solid and Structures 1984;20(3):277-297.

[2] Chandra R, Stemple AD, Chopra I. Thin-walled composite beams under bending, torsion, and extensional load. AIAA Journal, 1990;27(7):619-626.

[3] Cesnik CES, Hodges DH. VABS: A new concept for composite rotor blade cross-section modelling. Journal of the American Helicopter Society 1997;42(1):27-38.

[4] Lee J. Center of gravity and shear center of thin-walled open-section composite beam. Composite Structures 2001;52:255-260.
[5] Jung, SN, Nagaraj VT, Chopra I. Refined structural model for thin and thick walled composite rotor blades. AIAA Journal 2002;40(1):105-116.
[6] Kollar LP, Springer GS. Mechanics of composite structures, 1st edition. Cambridge University Press, 2003.
[7] Salim HA, Devalos JF. Torsion of open and closed thin-walled laminated composite sections. Journal of composite materials 2005;39(6):497-524.
[8] Lee J. Flexural analysis of thin-walled composite beams using shear-deformable beam theory. Composite Structures 2005;70(2):212-222.
[9] Shan. L, Qiao P. Flexural-torsional buckling of fiber-reinforced plastic composite open channel beam. Composite Structures 2005;68:211-224.
[10] Librescu L, Song O. Thin-walled composite beams, 1st edition. Springer, 2006.
[11] Berdichevsky VL. Variational-asymptotic method of constructing a theory of shell. PMM 1979;43(4):664-687.
[12] Volovoi VV, Hodges DH, Berdichevsky VL, Sutyrin V. Asymptotic theory for static behavior of elastic anisotropic I-beams. International Journal of Solids and Structures 1999;36:1017-1043.
[13] Volovoi VV, Hodges DH. Theory of anisotropic thin-walled beams. Journal of Applied Mechanics 2000;67:453-459.
[14] Volovoi VV, Hodges DH, Cesnik CES, Popescu B. Assessment of beam modeling methods for rotor blade applications. Mathematical and Computer Modelling 2001;33: 1099-1112.
[15] Volovoi VV, Hodges DH Single-and multi-celled composite thin-walled beams. AIAA Journal 2002;40:960-965.
[16] Yu W, Hodges DH, Volovoi VV, Fuchs ED. A generalized Vlasov theory for composite beams. Thin-Walled Structures 2005;43:1493-1511.
[17] Sheikh AH. A new concept to include shear deformation in a curved beam element. Journal of Structural Engineering, ASCE 2002;128(3):406-410.
[18] Reddy JN. Mechanics of laminated composite plates and shells: theory and analysis, 2nd edition. CRC Press, 2004.
[19] Lee J, Lee S. Flexural-torsional behavior of thin-walled composite beams. Thin-Walled Structures 2004;42(9):1293-1305.
[20] ABAQUS/Standard User's Manual, Version 6.1. Hibbit, Kalsson & Sorensen Inc. 2003.
[21] Vo TP, Lee J. Flexural-torsional behavior of thin-walled closed-section composite box beams. Engineering Structures 2007 (available online).
[22] Chandra R, Chopra I. Experimental and theoretical analysis of composite I beams with elastic couplings. AIAA Journal 1991;29(12):2197-2206.
[23] Smith EC, Chopra I. Formulation and evaluation of an analytical model for composite box-beams. Journal of the American Helicopter Society 1991;36(3):23-35.
[24] Stemple AD, Lee SW. A finite element model for composite beams with arbitrary cross-sectional warping. AIAA Journal. 1988;26(12):1512-1520.
[25] Kim NI, Shin DK, Kim MY. Exact solution for thin-walled open-section composite beams with arbitrary lamination subjected to torsional moment. Thin-Walled Structures 2006;44(6):638-654.

Appendix A

The explicit expressions for the elements of the matrix [C] found in Eq. (16) are presented in this Appendix. The matrix [C] is valid for all the three sections considered in this study. As the matrix is symmetric, the elements in the upper triangle of the matrix are listed below.

$C_{11} = A_{11}$, $C_{12} = yA_{11} - B_{11}\sin\alpha$, $C_{13} = z\,A_{11} + B_{11}\cos\alpha$, $C_{14} = \varphi A_{11} - qB_{11}$,
$C_{15} = -2B_{16} - A_{16}\left(r - \varphi_{,s}\right)$, $C_{16} = A_{16}\cos\alpha$, $C_{17} = A_{16}\sin\alpha$,
$C_{22} = y^2 A_{11} - 2yB_{11}\sin\alpha + D_{11}\sin^2\alpha$, $C_{23} = y\,z\,A_{11} + \left(y\cos\alpha - z\sin\alpha\right)B_{11} - D_{11}\sin\alpha\,\cos\alpha$,
$C_{24} = \varphi\,y\,A_{11} - \left(yq + \varphi\sin\alpha\right)B_{11} + qD_{11}\sin\alpha$,
$C_{25} = -A_{16}\left(r - \varphi_{,s}\right)y - B_{16}\left\{2y - \left(r - \varphi_{,s}\right)\sin\alpha\right\} + 2D_{16}\sin\alpha$, $C_{26} = yA_{16}\cos\alpha - B_{16}\sin\alpha\cos\alpha$,
$C_{27} = yA_{16}\sin\alpha - B_{16}\sin^2\alpha$,
$C_{33} = z^2\,A_{11} + 2zB_{11}\cos\alpha + D_{11}\cos^2\alpha$, $C_{34} = \varphi\,z\,A_{11} - \left(zq - \varphi\cos\alpha\right)B_{11} - qD_{11}\cos\alpha$,
$C_{35} = -A_{16}\left(r - \varphi_{,s}\right)z - B_{16}\left\{2z + \left(r - \varphi_{,s}\right)\cos\alpha\right\} - 2D_{16}\cos\alpha$, $C_{36} = z\,A_{16}\cos\alpha + B_{16}\cos^2\alpha$,
$C_{37} = z\,A_{16}\sin\alpha + B_{16}\sin\alpha\,\cos\alpha$,
$C_{44} = \varphi^2\,A_{11} - 2q\varphi B_{11} + q^2 D_{11}$, $C_{45} = -A_{16}\varphi\left(r - \varphi_{,s}\right) - B_{16}\left\{2\varphi - q\left(r - \varphi_{,s}\right)\right\} + 2qD_{16}$,
$C_{46} = \left(\varphi A_{16} - qB_{16}\right)\cos\alpha$, $C_{47} = \left(\varphi A_{16} - qB_{16}\right)\sin\alpha$
$C_{55} = \left(r - \varphi_{,s}\right)^2 A_{66} + 4B_{66}\left(r - \varphi_{,s}\right) + 4D_{66}$, $C_{56} = -A_{66}\left(r - \varphi_{,s}\right)\cos\alpha - 2B_{66}\cos\alpha$,
$C_{57} = -A_{66}\left(r - \varphi_{,s}\right)\sin\alpha - 2B_{66}\sin\alpha$
$C_{66} = A_{66}\cos^2\alpha + A_{55}\sin^2\alpha$, $C_{67} = \left(A_{66} - A_{55}\right)\sin\alpha\,\cos\alpha$
$C_{77} = A_{66}\sin^2\alpha + A_{55}\cos^2\alpha$

where $A_{ij} = \int Q_{ij}dn$, $B_{ij} = \int Q_{ij}n\,dn$ and $D_{ij} = \int Q_{ij}n^2 dn$

Appendix B

For the open section I profile as shown in Fig. 10, the warping function may be expressed as $\varphi = yz$. Based on this the expressions for the elements in the upper triangle of the symmetric matrix [F] found in Eq. (16) are as follows.

$F_{11} = b\left(A_{11}^1 + A_{11}^2\right) + d\,A_{11}^3$, $F_{12} = -d\,B_{11}^3$, $F_{13} = bd\left(A_{11}^1 - A_{11}^2\right)/2 + b\left(B_{11}^1 - B_{11}^2\right)$,
$F_{14} = 0$, $F_{15} = -2b\left(B_{16}^1 + B_{16}^2\right) - 2d\,B_{16}^3$, $F_{16} = b\left(A_{16}^1 - A_{16}^2\right)$, $F_{17} = d\,A_{16}^3$,
$F_{22} = b^3\left(A_{11}^1 + A_{11}^2\right)/12 + d\,D_{11}^3$, $F_{23} = 0$, $F_{24} = b^3 d\left(A_{11}^1 - A_{11}^2\right)/24 - b^3\left(B_{11}^1 - B_{11}^2\right)/12$,
$F_{25} = 2d\,D_{16}^3$, $F_{26} = 0$, $F_{27} = -d\,B_{16}^3$,
$F_{33} = bd^2\left(A_{111}^1 + A_{11}^2\right)/4 + d^3 A_{11}^3/12 + bd\left(B_{11}^1 + B_{11}^2\right) + b\left(D_{11}^1 + D_{11}^2\right)$, $F_{34} = -d^3 B_{11}^3/12$,
$F_{35} = -bd\left(B_{16}^1 - B_{16}^2\right) - 2b\left(D_{16}^1 - D_{16}^2\right)$, $F_{36} = bd\left(A_{16}^1 + A_{16}^2\right)/2 + b\left(B_{16}^1 + B_{16}^2\right)$, $F_{37} = 0$,
$F_{44} = b^3 d^2\left(A_{11}^1 + A_{11}^2\right)/48 - b^3 d\left(B_{11}^1 + B_{11}^2\right)/12 + b^3\left(D_{11}^1 + D_{11}^2\right)/12 + d^3 D_{11}^3/12$, $F_{45} = 0$, $F_{46} = 0$,
$F_{47} = 0$,
$F_{55} = 4b\left(D_{66}^1 + D_{66}^2\right) + 4d\,D_{66}^3$, $F_{56} = -2b\left(B_{66}^1 - B_{66}^2\right)$, $F_{57} = -2d\,B_{66}^3$

$$F_{66} = b\left(A_{66}^1 + A_{66}^2\right) + d\,A_{55}^3,\ F_{67} = 0$$
$$F_{77} = d\,A_{66}^3 + b\left(A_{55}^1 + A_{55}^2\right)$$

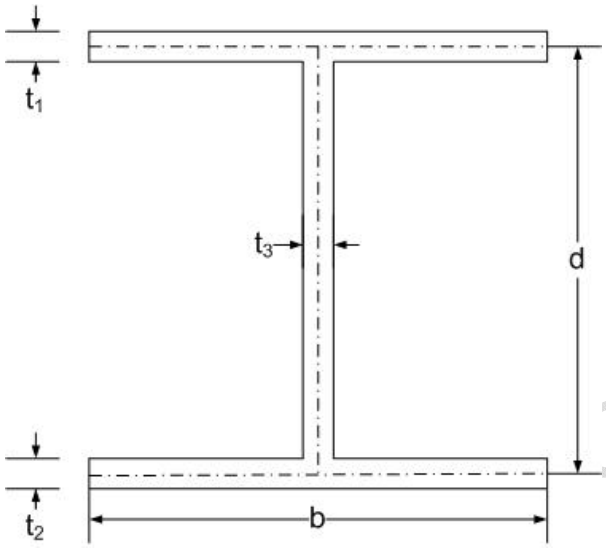

Fig. 10. Cross-sectional profile of the I beam

Appendix C

For the open section channel profile as shown in Fig. 11, the warping function may be expressed as $\varphi = z\left(y - e + y_d\right)$, where the location of the centroid [4] and shear centre [9] are:

$$y_d = \frac{\left(A_{11}^1 + A_{11}^2\right)b^2 - 2B_{11}^3 d}{2\left(A_{11}^1 b + A_{11}^2 b + A_{11}^3 d\right)} \text{ and } e = \frac{3t_3\left(A_{11}^1 b\right)^2}{t_1 A_{11}^3\left(A_{11}^3 d + 6A_{11}^1 b\right)}$$

With the above quantities, the elements of the matrix [F] are expressed as follows.

$$F_{11} = b\left(A_{11}^1 + A_{11}^2\right) + d\,A_{11}^3,\ F_{12} = by_b\left(A_{11}^1 + A_{11}^2\right) - dy_d A_{11}^3 - d\,B_{11}^3,$$
$$F_{13} = bd\left(A_{11}^1 - A_{11}^2\right)/2 + b\left(B_{11}^1 - B_{11}^2\right),\ F_{14} = bd\left(b - y_b - y_p\right)\left(A_{11}^1 - A_{11}^2\right)/2 - b\left(y_p + y_b\right)\left(B_{11}^1 - B_{11}^2\right),$$
$$F_{15} = -2b\left(B_{16}^1 + B_{16}^2\right) - 2d\,B_{16}^3,\ F_{16} = b\left(A_{16}^1 - A_{16}^2\right),\ F_{17} = d\,A_{16}^3,$$
$$F_{22} = \left(b^3/12 + by_b^2\right)\left(A_{11}^1 + A_{11}^2\right) + dy_d^2 A_{11}^3 + 2dy_d B_{11}^3 + d\,D_{11}^3,$$
$$F_{23} = b\,d\,y_b\left(A_{11}^1 - A_{11}^2\right)/2 + by_b\left(B_{11}^1 - B_{11}^2\right),$$
$$F_{24} = bd\left\{b^2/12 + y_b^2 - y_b\left(y_p - 2y_d\right)\right\}\left(A_{11}^1 - A_{11}^2\right)/2 - b\left(b^2/12 + y_b^2 + y_b y_p\right)\left(B_{11}^1 - B_{11}^2\right),$$
$$F_{25} = -2by_b\left(B_{16}^1 + B_{16}^2\right) + 2dy_d B_{16}^3 + 2d\,D_{16}^3,\ F_{26} = by_b\left(A_{16}^1 - A_{16}^2\right),\ F_{27} = -dy_d A_{16}^3 - d\,B_{16}^3,$$
$$F_{33} = bd^2\left(A_{11}^1 + A_{11}^2\right)/4 + d^3 A_{11}^3/12 + bd\left(B_{11}^1 + B_{11}^2\right) + b\left(D_{11}^1 + D_{11}^2\right),$$
$$F_{34} = b\,d^2\left(b - y_b - y_p\right)\left(A_{11}^1 + A_{11}^2\right)/4 + d^3\left(y_d - y_p\right)A_{11}^3/12 - b\,d\left(y_b + y_p - b/2\right)\left(B_{11}^1 + B_{11}^2\right)$$
$$- d^3 B_{11}^3/12 - b\left(y_b + y_p\right)\left(D_{11}^1 + D_{11}^2\right),\ F_{35} = -bd\left(B_{16}^1 - B_{16}^2\right) - 2b\left(D_{16}^1 + D_{16}^2\right),$$
$$F_{36} = bd\left(A_{16}^1 + A_{16}^2\right)/2 + b\left(B_{16}^1 + B_{16}^2\right),\ F_{37} = 0,$$
$$F_{44} = bd^2\left\{b^2/12 + y_b^2 - 2y_b\left(y_p - 2y_d\right) + \left(y_p - 2y_d\right)^2\right\}\left(A_{11}^1 + A_{11}^2\right)/4 + d^3\left(y_p - y_d\right)^2 A_{11}^3/12$$

$$-bd\left\{b^2/12+y_b^2+2y_by_d-y_p\left(y_p-2y_d\right)\right\}\left(B_{11}^1+B_{11}^2\right)+d^3\left(y_p-y_d\right)B_{11}^3/6$$
$$+b\left(b^2/12+y_b^2+2y_by_p+y_p^2\right)\left(D_{11}^1+D_{11}^2\right)+d^3D_{11}^3/12,$$
$$F_{45}=-d\left(b-y_b-y_p\right)\left(B_{16}^1-B_{16}^2\right)+2b\left(y_b+y_p\right)\left(D_{16}^1-D_{16}^2\right),$$
$$F_{46}=bd\left(b-y_b-y_p\right)\left(A_{16}^1+A_{16}^2\right)/2-b\left(y_b+y_p\right)\left(B_{16}^1+B_{16}^2\right),\ F_{47}=0,$$
$$F_{55}=4b\left(D_{66}^1+D_{66}^2\right)+4d\,D_{66}^3,\ F_{56}=-2b\left(B_{66}^1-B_{66}^2\right),\ F_{57}=-2d\,B_{66}^3,$$
$$F_{66}=b\left(A_{66}^1+A_{66}^2\right)+d\,A_{55}^3,\ F_{67}=0,\ F_{77}=b\left(A_{55}^1+A_{55}^2\right)+d\,A_{66}^3$$

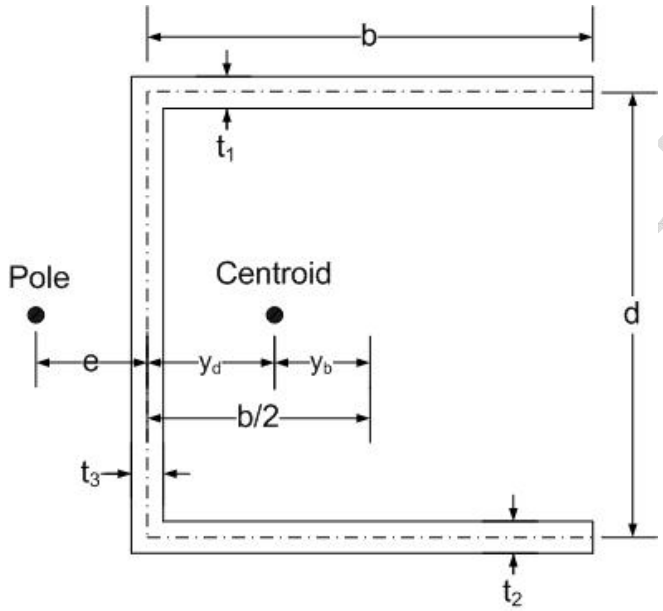

Fig. 11. Cross-sectional profile of the channel beam

Appendix D

For the closed section box profile as shown in Fig. 12, the warping function may be simply expressed as $\varphi=\beta yz$, where $\beta=(b-d)/(b+d)$ if all the walls are identical and placed symmetrically with respect to the centroid [2]. With this the elements of the matrix [F] may be expressed as follows.

$$F_{11}=b\left(A_{11}^1+A_{11}^2\right)+d\left(A_{11}^3+A_{11}^4\right),\ F_{12}=-bd\left(A_{11}^3-A_{11}^4\right)/2-d\left(B_{11}^3-B_{11}^4\right),$$
$$F_{13}=bd\left(A_{11}^1-A_{11}^2\right)/2+b\left(B_{11}^1-B_{11}^2\right),\ F_{14}=0,$$
$$F_{15}=-bd\left\{\left(A_{16}^1+A_{16}^2\right)(1-\beta)+\left(A_{16}^3+A_{16}^4\right)(1+\beta)\right\}/2-2b\left(B_{16}^1+B_{16}^2\right)-2d\left(B_{16}^3+B_{16}^4\right),$$
$$F_{16}=b\left(A_{16}^1-A_{16}^2\right),\ F_{17}=d\left(A_{16}^3-A_{16}^4\right),$$
$$F_{22}=b^3\left(A_{11}^1+A_{11}^2\right)/12+b^2d\left(A_{11}^3+A_{11}^4\right)/4+bd\left(B_{11}^3+B_{11}^4\right)+d\left(D_{11}^3+D_{11}^4\right),\ F_{23}=0,$$
$$F_{24}=\beta b^3d\left(A_{11}^1-A_{11}^2\right)/24-b^3\left(B_{11}^1-B_{11}^2\right)/12,$$
$$F_{25}=b^2d\,(1+\beta)\left(A_{16}^3-A_{16}^4\right)/4+bd\,(3+\beta)\left(B_{16}^3-A_{16}^4\right)/2+2d\left(D_{16}^3-D_{16}^4\right),\ F_{26}=0,$$
$$F_{27}=-bd\left(A_{16}^3+A_{16}^4\right)/2-d\left(B_{16}^3+B_{16}^4\right),$$

$$F_{33} = bd^2\left(A_{11}^1 + A_{11}^2\right)/4 + d^3\left(A_{11}^3 + A_{11}^4\right)/12 + bd\left(B_{11}^1 + B_{11}^2\right) + b\left(D_{11}^1 + D_{11}^2\right),$$
$$F_{34} = -\beta bd^3\left(A_{11}^3 - A_{11}^4\right)/24 - d^3\left(B_{11}^3 - B_{11}^4\right)/12\ ,$$
$$F_{35} = -bd^2(1-\beta)\left(A_{16}^1 - A_{16}^2\right)/4 - bd(3-\beta)\left(B_{16}^1 - B_{16}^2\right)/2 - 2b\left(D_{16}^1 - D_{16}^2\right),$$
$$F_{36} = bd\left(A_{16}^1 + A_{16}^2\right)/2 + b\left(B_{16}^1 + B_{16}^2\right),\ F_{37} = 0\ ,$$
$$F_{44} = \beta^2 b^3 d^2\left(A_{11}^1 + A_{11}^2\right)/48 + \beta^2 b^2 d^3\left(A_{11}^3 + A_{11}^4\right)/48 - \beta b^3 d\left(B_{11}^1 + B_{11}^2\right)/12$$
$$+ \beta bd^3\left(B_{11}^3 + B_{11}^4\right)/12 + b^3\left(D_{11}^1 + D_{11}^2\right)/12 + d^3\left(D_{11}^3 + D_{11}^4\right)/12\ ,$$
$$F_{45} = 0\ ,\ F_{46} = 0\ ,\ F_{47} = 0\ ,$$
$$F_{55} = bd\left\{d(1-\beta)^2\left(A_{66}^1 + A_{66}^2\right) + b(1+\beta)^2\left(A_{66}^3 + A_{66}^4\right)\right\}/4$$
$$+ 2bd\left\{(1-\beta)\left(B_{66}^1 + B_{66}^2\right) + (1+\beta)\left(B_{66}^3 + B_{66}^4\right)\right\} + 4b\left(D_{66}^1 + D_{66}^2\right) + 4d\left(D_{66}^3 + D_{66}^4\right),$$
$$F_{56} = -bd(1-\beta)\left(A_{66}^1 - A_{66}^2\right)/2 - 2b\left(B_{66}^1 - B_{66}^2\right),\ \ F_{57} = -bd(1+\beta)\left(A_{66}^3 - A_{66}^4\right)/2 - 2d\left(B_{66}^3 - B_{66}^4\right),$$
$$F_{66} = b\left(A_{66}^1 + A_{66}^2\right) + d\left(A_{55}^3 + A_{55}^4\right),\ F_{67} = 0$$
$$F_{77} = b\left(A_{55}^1 + A_{55}^2\right) + d\left(A_{66}^3 + A_{66}^4\right)$$

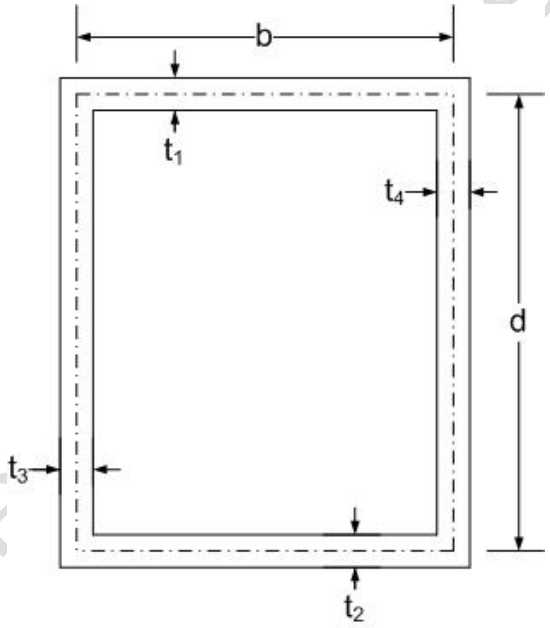

Fig. 12. Cross-sectional profile of the box beam